# Bioactivity-HiTES Unveils Cryptic Antibiotics Encoded in Actinomycete Bacteria

Kyuho Moon,[†] Fei Xu,[†] Chen Zhang,[†] and Mohammad R. Seyedsayamdost[*,†,‡]

[†]Department of Chemistry, Princeton University, Princeton, New Jersey 08544, United States
[‡]Department of Molecular Biology, Princeton University, Princeton, New Jersey 08544, United States

S *Supporting Information*

ABSTRACT: Bacteria harbor an immense reservoir of potentially new and therapeutic small molecules in the form of "silent" biosynthetic gene clusters (BGCs). These BGCs can be identified bioinformatically but are sparingly expressed under normal laboratory growth conditions, or not at all, and therefore do not produce significant levels of the corresponding small molecule product. Several methods have been developed for activating silent BGCs. A major limitation for nearly all methods is that they require genetic procedures and/or do not report on the bioactivity of the cryptic metabolite. We herein report "Bioactivty-HiTES", an approach that links the bioactivity of cryptic metabolites to their induction while at the same time obviating the need for genetic manipulations. Using this method, we detected induction of cryptic antibiotics in three actinomycete strains that were tested. Follow-up studies in one case allowed us to structurally elucidate two cryptic metabolites, elicited by the β-blocker atenolol in *Streptomyces hiroshimensis*, with selective growth-inhibitory activity against Gram-negative bacteria, notably *Escherichia coli* and *Acinetobacter baumannii*. Atenolol turned out to be a global elicitor of secondary metabolism, and characterization of additional cryptic metabolites led to the discovery of a novel naphthoquinone epoxide. Bioactivity-HiTES is a general, widely applicable procedure that will be useful in identifying cryptic bioactive metabolites in the future.
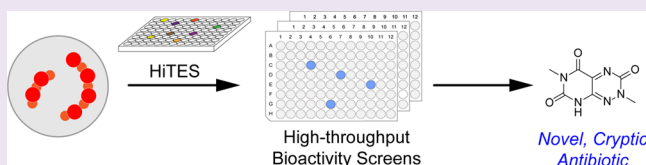
B acteria produce a diverse array of secondary metabolites, or natural products, the discovery of which has been an important driving force for various disciplines in chemistry, biology, and pharmacology.[1] Natural products account for >50% of the drugs approved by the Food and Drug Administration in the United States in the past ∼35 years and >70% of the current clinical antibiotics.[2−4] These data provide a strong impetus for the continued discovery and development of new natural products.

By the early 2000s, the secondary metabolic potential of well-known bacterial genera appeared to have been exhausted. Rediscovery of old molecules was a major bottleneck, leading to a sharp decline in natural product research in the pharmaceutical industry.[5−7] However, innovations that led to next-generation sequencing and the ensuing accumulation of thousands of complete bacterial genomes, along with advances in bioinformatic identification of biosynthetic genes, revealed that the biosynthetic potential of bacteria, even well-studied ones, had been vastly underestimated.[8−14] We now know that bacteria harbor many secondary metabolite biosynthetic gene clusters (BGCs) that do not give rise to appreciable levels of a small molecule product under normal laboratory conditions. These BGCs are termed "silent" or "cryptic", and the current consensus is that they outnumber constitutively active ones by a factor of 5−10. Silent BGCs, therefore, represent a massive reservoir of potentially new small molecules, the underlying chemistry and biology of which remain to be explored.

With the realization of the abundance of silent BGCs, feverish activity has followed to devise methods for harvesting cryptic metabolites.[15−19] We have contributed to the available approaches with our development of HiTES (high-throughput elicitor screening).[20,21] In this approach, a reporter gene is placed inside the gene cluster of interest and small molecule libraries are then screened against the reporter strain to find suitable transcriptional elicitors or inducers. With the inducer identified, the small molecule product can be characterized along with the regulation of the silent BGC, an area that remains largely in its infancy.[22] The disadvantage of HiTES and of most other available techniques is that genetic manipulations and/or molecular biology approaches are required. These slow the pace of discovery, especially in the talented but genetically intractable rare actinomycetes, which are prolific producers of secondary metabolites and harbor stores of silent BGCs.[12] A second drawback of most available approaches, with some notable exceptions,[23] is that they do not link bioactivity to a given cryptic metabolite or BGC. Therefore, activity assays must be conducted upon discovery of a cryptic metabolite. Given that natural products have a virtually unlimited potential for biological function, both in the environment and in medicine, a method that directly connects
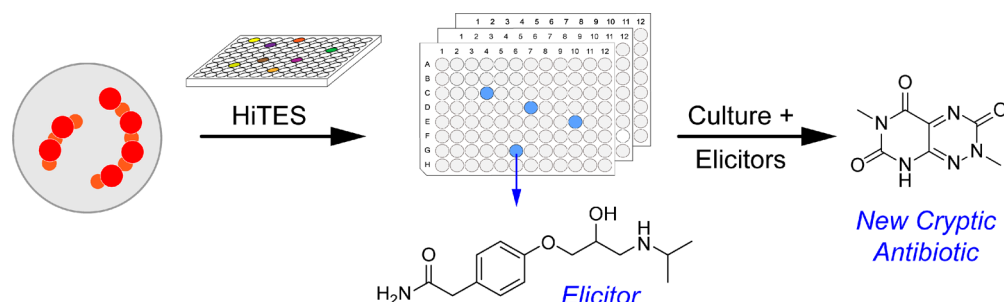
Figure 1. Summary of the Bioactivity-HiTES workflow. A wild-type microorganism is subjected to elicitor screening. Each well is then screened for a selected biological activity, such as antibiosis. The desired elicitor−cryptic metabolite pair is subsequently characterized.

bioactivity to a cryptic metabolite prior to its tedious isolation and structural elucidation would be highly beneficial.

We herein introduce "Bioactivity-HiTES", an approach that both addresses the limitations mentioned above and obviates the need for genetic manipulations by identifying cryptic metabolites with the desired bioactivity: a wild-type microorganism is subjected to elicitor screening in a high-throughput fashion. The resulting "induced metabolomes" are screened for a chosen bioactivity. Activity-guided fractionation in combination with the elicitor then allows for isolation and characterization of the cryptic metabolite. We demonstrate the feasibility of this approach by screening for cryptic antibiotics and report two pyrimidine natural products that are toxic to and mildly selective for Gram-negative bacteria. Follow-up studies allowed us to identify the cognate BGC along with other novel cryptic metabolites that are pleiotropically induced by the same elicitor, notably a novel pyranonaphthoquinone epoxide that we call hiroshidine.

■ RESULTS

Rationale for Bioactivity-HiTES. HiTES consists of two steps, the activation of silent BGCs by elicitor screening followed by a genetic readout, which so far has relied on transcriptional or translational reporter assays. Most recently, we have applied an imaging mass spectrometry approach as the detection step to remove the reliance on genetic procedures.[24] While cryptic bioactive metabolites can be, and have been, discovered with these approaches, neither reports directly on the bioactivity of the desired metabolite. To address this limitation, we considered a workflow in which a bacterium would be subjected to elicitor screening and the resulting ∼500−1000 induced metabolomes would be screened for a desired biological activity (Figure 1). Wells that contained the active component(s) would be pursued further to identify the cryptic metabolite of interest. Naturally, the approach can be applied only to bacteria that do not constitutively produce the chosen bioactivity. Because of the well-documented need for new antibiotics and the continuing development of resistance to extant ones, we focused on cryptic metabolites that exhibit inhibitory activity against Gram-positive (*Bacillus subtilis*) and Gram-negative (*Escherichia coli*) bacteria.

Development of Bioactivity-HiTES. We began by screening several actinomycete bacteria in our strain library, starting with *Streptomyces lavendulae*, *Amycolatopsis keratiniphila*, and *Streptomyces hiroshimensis*, the producers, among others, of streptothricin, keratinimicin, and prodigiosin, respectively. We verified that neither produced an antibiotic under our experimental conditions in R4 growth medium. We then subjected each strain to elicitor screening from a single

96-well plate of a larger, commercial natural product library. After growth of each strain under 80−96 different conditions, the supernatants were used directly in disc diffusion assays against *B. subtilis*. The resulting agar plates were assessed visually, and the frequency and size of growth-inhibition zones were tabulated. Somewhat surprisingly, even with this limited screen, we observed a number of conditions that gave rise to a zone of inhibition (Figure 2 and Figures S1−S3). Some of
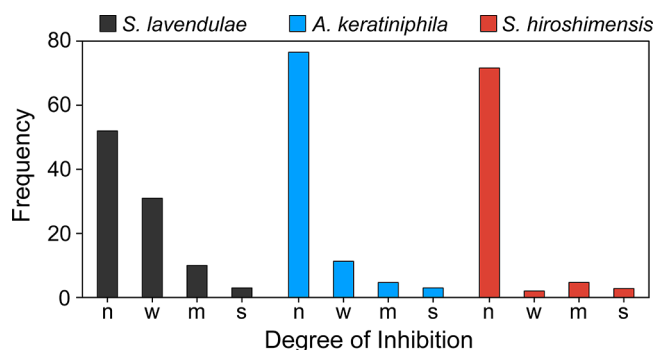

Figure 2. Identification of antibiotic-eliciting small molecules from three actinomycetes. Summary of results from agar plate assays in which *S. lavendulae*, *A. keratiniphila*, and *S. hiroshimensis* were challenged with 80−96 elicitors and the resulting metabolomes were screened for antibiotic activity against *B. subtilis*. The plates are shown in Figures S1−S3. The size of the zones of inhibition observed correspond to none (n), weak (w, 5−6 mm), medium (m, 6−7 mm), and strong (s, >7 mm).

these were likely the result of residual antibiotics from the natural product library, but in most cases, the elicitor was not known to exhibit antibiotic properties. For example, in *S. lavendulae*, 7,2′-dimethoxyflavone, isobutylmethylxanthine, and methoxyvone appeared to induce synthesis of anti-*B. subtilis* metabolite(s) (Figure S1). For *A. keratiniphila*, baccatin III and isoscopoletin gave rise to zones of inhibition that were otherwise not observed (Figure S2). Lastly, with *S. hiroshimensis*, several clinical drugs, including the antimalarial primaquine and the anesthetic procaine, appeared to elicit anti-*B. subtilis* metabolite(s) (Figure S3). The stimulatory activities of these metabolites had previously not been reported.

We also carried out assays against *E. coli*. In this case, we conducted broader elicitation screens using an ∼500-member natural product library as the source of potential inducers. To increase the throughput of the assays, we changed to liquid bioassays. Rather than manually spotting each disc, we robotically transferred the supernatant from the elicitor plate to 96-well plates inoculated with the *E. coli* test strain. After a

defined period, growth inhibition was assessed by monitoring the optical density at 600 nm (OD_{600}) using a plate reader. To account for growth variation from one plate to another, the percent growth for each well was plotted, that is, the OD_{600} in the presence of an elicitor relative to the average OD_{600} for all the wells in a given plate. The results for the entire library are shown for *S. lavendulae* (Figure 3A), *A. keratiniphila* (Figure 3B), and *S. hiroshimensis* (Figure 3C). Most wells gave a value close to 100 ± 30%, suggesting a minimal effect on growth. Some induced metabolomes enhanced *E. coli* growth, while others inhibited it. With *S. lavendulae*, metabolomes induced by the heart block agent isoproterenol and the bile acid chenodiol seemed to support *E. coli* growth best, while those induced by inositol and allantoin inhibited it (blue and red spheres, Figure 3A). Similarly, aspartame- and tandutinib-induced metabolomes of *A. keratiniphila* resulted in enhanced *E. coli* growth, while those induced by the anti-HIV medication AZT and the antipsychotic sulpiride seemed to produce growth-inhibitory compounds (blue and red spheres, Figure 3B). Lastly, with *S. hiroshimensis*, the metabolomes that most enhanced *E. coli* growth were elicited by aceclidine (Figure 3D, **1**), an acetylcholine agonist used to treat glaucoma, glucosamine (**2**), and dexchlorpheniramine (**3**), a clinical antihistamine. The metabolomes that resulted in the lowest percent growth, and inhibited *E. coli* growth best, were induced by atenolol (Figure 3D, **4**), a β-blocker clinically used to treat hypertension, the Alzheimer drug memantine (**5**), and the ergot alkaloid methylergonovine (**6**). These results provide ample opportunities for follow-up studies to investigate the effects of these unsuspected modulators of actinomycete physiology.

Discovery of New, Cryptic Antibiotics. The observation of numerous conditions that seem to elicit biomolecules with growth-inhibitory activities suggests that cryptic antibiotics can be identified using Bioactivity-HiTES. Because of the dearth of treatments against Gram-negative bacteria, we next sought to verify production of cryptic metabolites that inhibit *E. coli* growth. To do so, we focused on *S. hiroshimensis*, because relatively few studies have investigated its natural product output. The atenolol-induced metabolome was most effective at inhibiting *E. coli*, and further experiments were carried out with this elicitor. We validated the effects of atenolol using disc diffusion assays and high-performance liquid chromatography−mass spectrometry (HPLC−MS) analysis. *S. hiroshimensis* culture supernatants induced by atenolol resulted in a clear zone of inhibition on *E. coli* agar plates and an orange hue, while uninduced cultures exhibited neither (Figure 4A). Moreover, differential HPLC−MS profiling revealed numerous new peaks induced by the β-blocker, indicative of global induction of secondary metabolism (Figure 4B). Much like other elicitors that we have explored in the past, atenolol too appears to have a pleiotropic effect on secondary metabolism in *S. hiroshimensis*.[20−22]

We set out to determine the cryptic anti-*E. coli* antibiotic that was induced by atenolol and elucidate the structures of the additional cryptic metabolites. Bioactivity assays of the induced peaks showed that the antibiotic activity was associated with compounds **7** and **8** (Figure 4B). Large-scale production cultures in the presence of atenolol followed by activity-guided fractionation allowed us to purify two related metabolites. HR-MS suggested that both compounds were nitrogen-rich with predicted molecular formulas of $C_7H_7N_5O_3$ and $C_8H_9N_5O_3$ (Table S1). Ultraviolet−visible (λ_{max} ∼ 240 and 420 nm) and
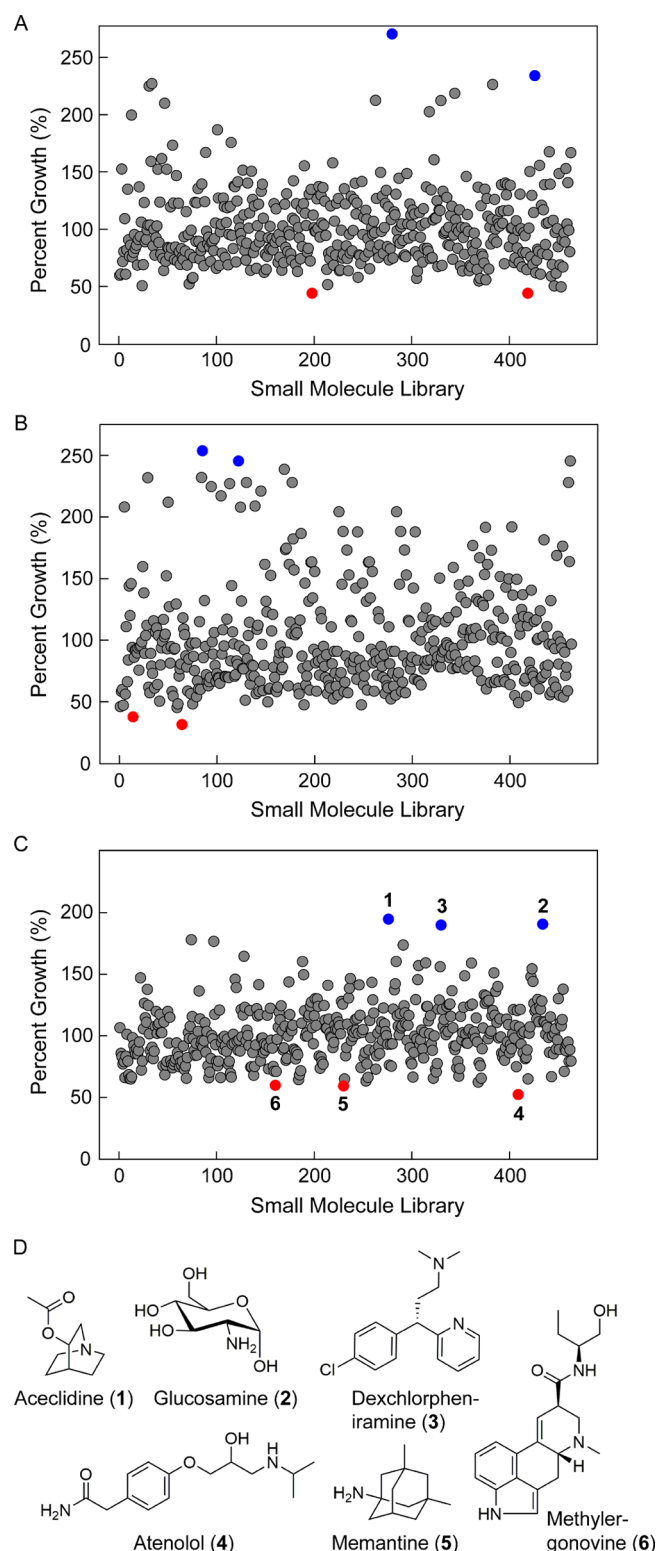

Figure 3. Cryptic metabolites with inhibitory bioactivity against *E. coli*. (A−C) Bioactivity-HiTES of *S. lavendulae*, *A. keratiniphila*, and *S. hiroshimensis*, respectively, against *E. coli*. Each bacterium was challenged with an ∼500-member natural product library. After a suitable growth period, the supernatants from each of the ∼500 wells were transferred to 96-well plates inoculated with *E. coli*, the plates were cultured for a defined period, and OD_{600} was subsequently recorded. For each well, percent growth, that is, the OD_{600} for a given well relative to the average OD_{600} for the entire plate, was calculated and plotted. This normalization eliminated differences in growth

Figure 3. continued

kinetics that can arise from plate-to-plate variation. With *S. lavendulae* and *A. keratiniphila*, the two wells that stimulated (blue dots) or inhibited (red dots) *E. coli* growth most are highlighted. With *S. hiroshimensis*, the three wells that resulted in the optimal stimulation (**1**−**3**, blue circles) or inhibition (**4**−**6**, red circles) of *E. coli* growth are marked. (D) Structures of elicitors **1**−**6** from Bioactivity-HiTES with *S. hiroshimensis*.

nuclear magnetic resonance (NMR) analyses were in line with a 7-azapteridine scaffold with three ketone carbon shifts at 149.8, 153.2, and 158.4 ppm in the first analogue as well as two

N-methyl groups with ^{1}H shifts at 3.22 and 3.67 ppm (Figure S4). Detailed analysis of one- and two-dimensional NMR data ultimately revealed that the two compounds consisted of a new toxoflavin-type analogue (**7**) and 2-methylfervenulone (**8**), a metabolite that was previously isolated from an unidentified actinomycete (Table S2 and Figures S4 and S5).[25,26] Interestingly, compound **8** and a series of other pyrimidine natural products were synthesized by Taylor and colleagues, a research program that culminated in the drug Alimta.[27,28] We have therefore named these pyrimidine compounds taylorflavin A (Figure 4C, **7**) and B (**8**), in honor of Ted Taylor.
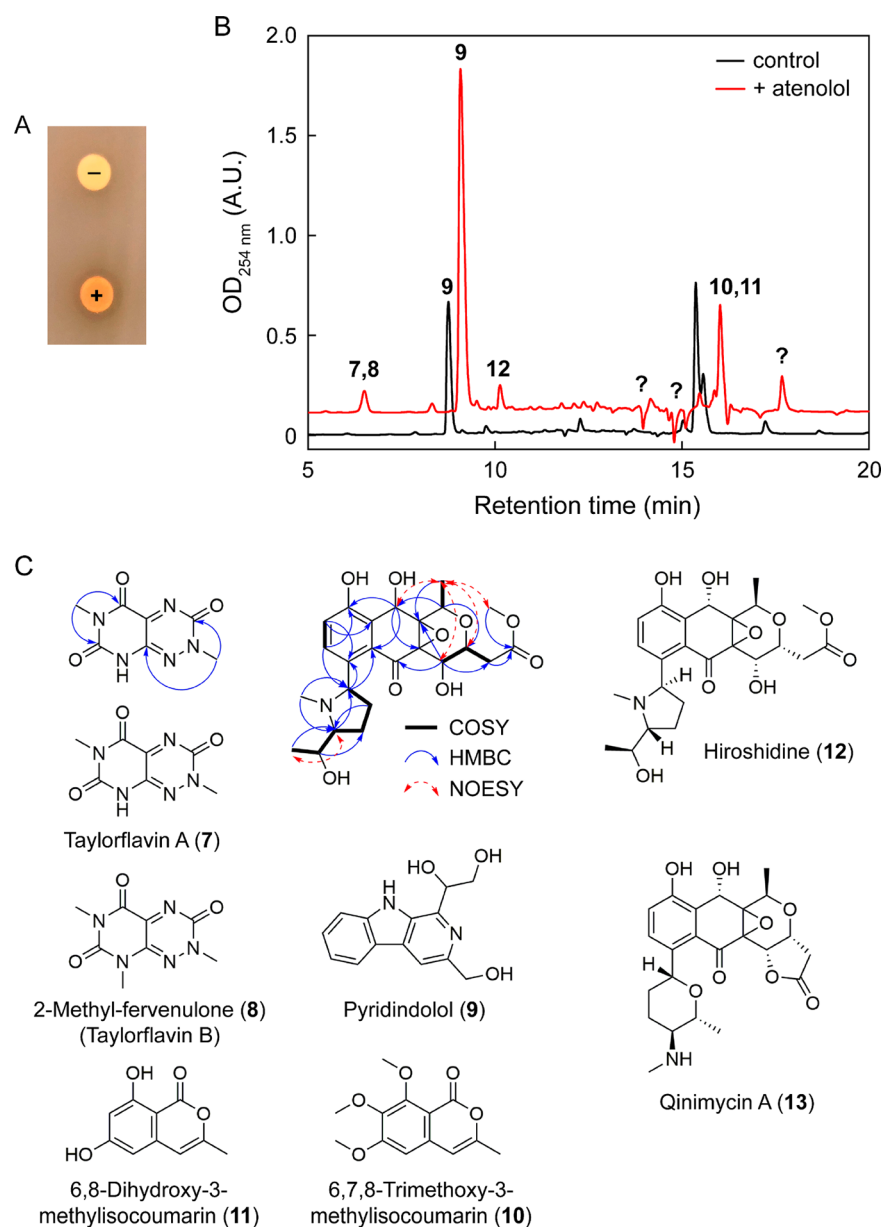

Figure 4. Identification of cryptic metabolites induced by atenolol. (A) Agar disc diffusion assays of uninduced (−) and atenolol-induced (+) *S. hiroshimensis* cultures against *E. coli*, verifying the induction of compounds with growth-inhibitory activity against *E. coli*. (B) Comparative HPLC-MS profile of *S. hiroshimensis* cultures grown in the absence (black trace) or presence (red trace) of 33 μM atenolol. Identified peaks are numbered with the structures shown in panel C. Note that compounds **7**/**8** and **10**/**11** had similar retention times. Several newly induced metabolites remain unidentified (question mark). (C) Taylorflavins, pyridindolol, two isocoumarins, and hiroshidine were identified from atenolol-induced *S. hiroshimensis* cultures. Relevant nuclear magnetic resonance data for taylorflavin A and hiroshidine are shown. Qinimycin A is the closest structural homologue of hiroshidine.

In-house bioactivity assays showed taylorflavin B to be a more potent inhibitor of *E. coli* growth. We submitted this compound for broad bioactivity assays against a battery of pathogenic bacteria; a more limited set was tested with taylorflavin A. Consistent with our screen, the results yielded minimal inhibitory concentrations (MICs) of 4 μg/mL against *Neisseria ghonorrheae* and 16 μg/mL against *E. coli*, *Acinetobacter baumannii*, and *Vibrio cholerae* for taylorflavin B (Table 1). Conversely, the antibiotic did not inhibit the growth

Table 1. MIC Values (micrograms per milliliter) of Taylorflavins against Select Bacteria[a]

bacterium	taylorflavin A	taylorflavin B
Gram-negative		
E. coli	37.5	**16**
A. baumannii	nd	**16**
V. cholerae	nd	**16**
N. gonorrhoeae	nd	**4**
P. aeruginosa	**25**	>64
Klebsiella pneumoniae	nd	>64
Gram-positive		
St. aureus	>64	64
St. aureus MRSA	nd	64
Streptococcus pneumoniae PSPP	nd	32
Streptococcus pyogenes	nd	32
Streptococcus agalactiae	nd	32
Enterococcus faecalis VSE	nd	>64
En. faecalis VRE	nd	64
B. subtilis	>64	64
Clostridium difficile	nd	>64
Bacillus fragilis	nd	>64

[a]See the Supporting Information for details. Significant bioactivities (MIC $\leq$ 25 μg/mL) are shown in bold. nd; not determined.

of a collection of Gram-positive bacteria. Likewise, taylorflavin A displayed MICs of 25 and 37.5 μg/mL against *Pseudomonas aeruginosa* and *E. coli*, respectively. Significantly weaker activity was observed against *B. subtilis* and *Staphylococcus aureus* (Table 1). In contrast to most antibiotics, the taylorflavins exhibited Gram-negative-selective antibacterial activity. These results validate the use of Bioactivity-HiTES for the discovery of cryptic antibiotics.

Pleiotropic Stimulation of Secondary Metabolism. Differential metabolic profiling shows that atenolol is not a specific inducer of the toxoflavin-like pteridines but rather a global elicitor of secondary metabolism (Figure 4B). As few metabolites have been reported from *S. hiroshimensis*, we characterized the additional compounds observed in the presence of atenolol. One- and two-dimensional NMR and/or HR-MS identified one of these, produced under normal conditions but further induced by atenolol, as pyridindolol (Figure 4C, **9**), a secondary metabolite previously isolated from *Streptomyces alboverticillatus* with inhibitory activity against β-galactosidase (Table S1 and Figure S6).[29] Two further metabolites, whose production was also enhanced by atenolol, were determined to be 6,7,8-trimethoxy-3-methyl-isocoumarin (**10**) and 6,8-dihydroxy-3-methylisocoumarin (**11**), previously isolated from *Streptomyces* sp. ANK302 with zoosporicidal, but lacking antibacterial, bioactivity (Figures S6 and S7 and Table S3).[30] Lastly, we focused on peak **12** (Figure 4C). Initial analysis by HR-MS and comparison with a database of known natural products indicated that it was likely

new. Structural elucidation by one- and two-dimensional NMR revealed a naphthoquinone-type scaffold that was fused to a substituted tetrahydropyran group. ^{13}C and HMBC shifts were consistent with the presence of an epoxide group bridging the pyrano and naphthoquinone moieties, with characteristic ^{13}C shifts at 61.9 and 66.8 ppm (Figures S8 and S9). The naphthoquinone was modified with a spin system containing a contiguous, substituted -CH-CH$_2$-CH$_2$-CH-CH-CH$_3$- chain as revealed by COSY spectra. HSQC and HMBC analysis indicated it consisted of an *N*-methyl-1-hydroxyethyl-substitued pyrrolidine, thus completing the two-dimensional structure of the compound, to which we have assigned the trivial name hiroshidine (Figure 4C, **12**, and Table S3).

Hiroshidine's structure is closest to that of qinimycin A (**13**), recently identified by the van Wezel group from *Streptomyces* sp. MBT76.[31] It contains nine stereocenters. Preliminary attempts to crystallize hiroshidine failed. On the basis of NMR NOESY constraints, we propose the relative stereochemistry shown for some of the stereocenters (Figure 4C). Further work is required to experimentally assign the absolute stereochemistry at these positions as well as that of the epoxide group in hiroshidine.

Biosynthetic Gene Clusters for Taylorflavins and Hiroshidine. Given the unusual structural features of taylorflavins and hiroshidine, we investigated the BGCs for the two groups of metabolites. We suspected that taylorflavins may follow a biosynthetic pathway similar to that of toxoflavin, which has been shown to be composed of GTP and Gly.[32−34] Indeed, growth of *S. hiroshimensis* in the presence of atenolol and 2-^{13}C-Gly revealed taylorflavins that were now 1 Da heavier, consistent with incorporation of Gly (Table S1). This result suggested that we could identify the taylorflavin cluster by scouring the genome of *S. hiroshimensis* for genes encoded in the toxoflavin cluster (*tox*).

To find a *tox*-like cluster, the genome sequence of *S. hiroshimensis* was determined with 70-fold coverage using Illumina sequencing technology, resulting in a single chromosome at 8.4 Mbp. Analysis by antiSMASH revealed a total of 47 BGCs, suggesting that *S. hiroshimensis* harbors a prolific potential for secondary metabolite synthesis. The BGC of toxoflavin has been characterized in *Burkholderia glumae* and *Pseudomonas protegens*, and the reactions of some of the enzymes have been examined *in vitro*.[32−34] The biosynthetic pathway begins with the action of a GTP cyclohydrolase encoded by *toxB*. We searched the genome of *S. hiroshimensis* using *toxB* from *P. protegens* Pf-5 as a query and obtained a single hit. Several genes involved in toxoflavin biosynthesis could be identified, including *toxA* (SAM-dependent methyltransferase), *toxC* (WD40-repeat protein with yet unknown function), and *toxE* (a *ribD* homologue) (Figure 5A and Table S4). Unique to this cluster were a second putative SAM-dependent methyltransferase (*tflA*), a Ser/Thr kinase (*tflB*), an open reading frame lacking similarity to known proteins (*tflC*), an oxidoreductase (*tflD*), possibly involved in introduction of the additional carbonyl functionality, and a transcriptional regulator (*tflE*).

To find the hiroshidine BGC, we used a type II polyketide synthase (PKS) from the qinimycin gene cluster (*qin*) in *Streptomyces* sp. MBT76 as a query.[31] Again, we obtained a single hit inside an ~40 kb gene cluster, containing many of the same genes as the *qin* BGC. This cluster, which we annotate as *hrs*, is significantly smaller than *qin* but encodes type II PKSs as well as a number of genes involved in sugar
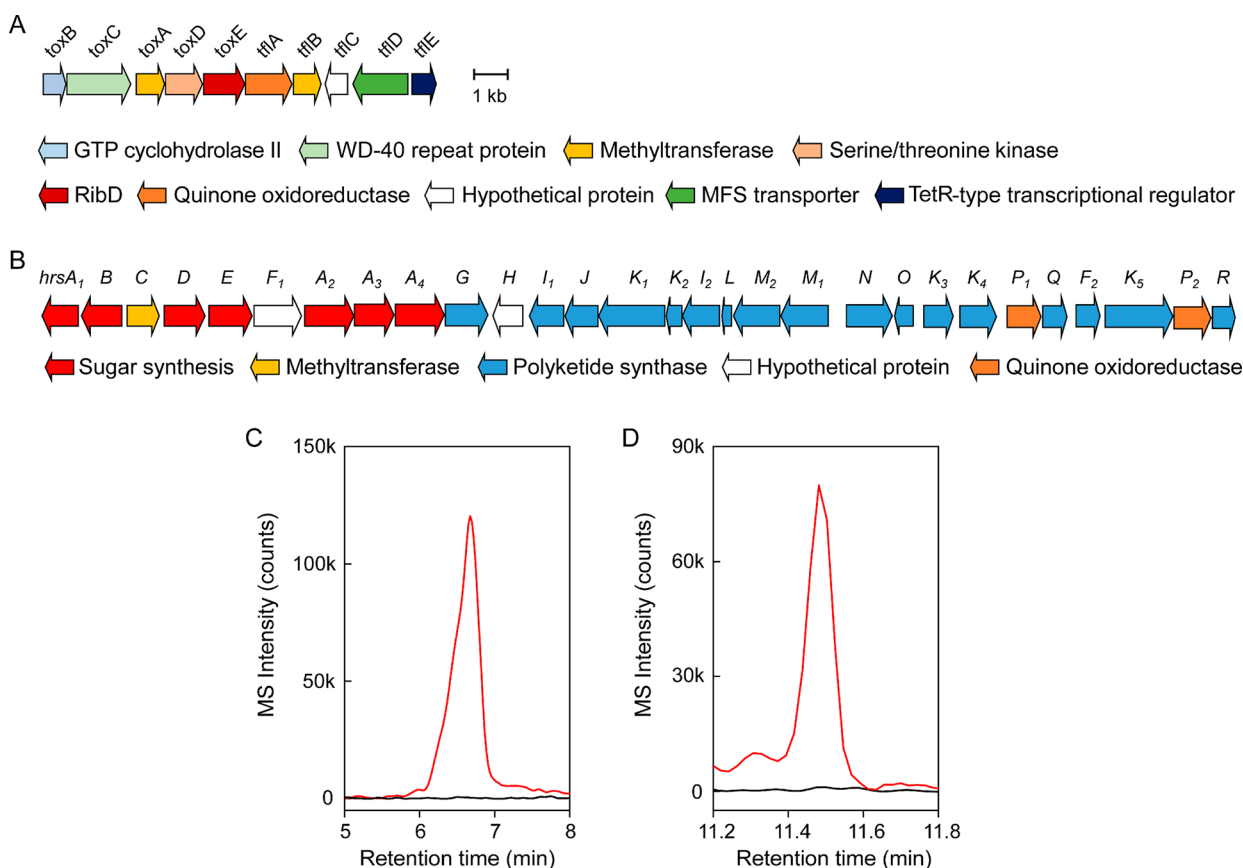
Figure 5. Biosynthetic gene clusters for taylorflavins and hiroshidine. (A) The *tfl/tox* BGC consists of genes *tflABCDE* as well as *toxABCDE*, which are shared with the *tox* gene cluster. (B) The *hrs* gene cluster is homologous to *qin* and primarily encodes sugar and polyketide biosynthetic enzymes. (C) Extracted ion chromatogram for taylorflavin B (m/z 224.1) in wild-type (red trace) and *toxB−tflA::apr* (black trace) *S. hiroshimensis* cultures. (D) Extracted ion chromatogram for hiroshidine (m/z 478.2) in wild-type (red trace) and *hrsC−hrsJ::apr* (black trace) *S. hiroshimensis* cultures.

biosynthesis and other modifications (Figure 4B and Table S5). A biosynthetic pathway for qinimycin has been proposed but awaits experimental verification.[31]

We used a genetic approach to verify that the two gene clusters *tfl/tox* and *hrs* encode taylorflavins and hiroshidine. The *tfl/tox* locus was inactivated by replacing the six genes between *toxB* and *tflA* with an apramycin resistance gene (*apr*) using insertional mutagenesis, thus giving rise to a *toxB−tflA::apr* mutant strain (see the Methods in the Supporting Information and Table S6). Likewise, *hrsC−hrsJ::apr* was generated to investigate the role of the *hrs* BGC in hiroshidine production. The wild type and both mutants were subsequently cultured in the presence of atenolol, and the supernatants examined by HPLC−MS. In the wild type, we could clearly see production of both metabolites. In the *toxB−tflA::apr* strain, production of taylorflavins was abolished (Figure 4C), though hiroshidine was observed under these conditions (Figure S10). Similarly, hiroshidine was not observed in the *hrsC−hrsJ::apr* strain, though it was induced in the wild-type and *toxB−tflA::apr* strains in response to atenolol (Figure 4D and Figure S10). These results are consistent with a role for the *tfl/tox* and *hrs* clusters in biosynthesizing taylorflavins and hiroshidine, respectively. With the BGCs identified, future studies will be able to assess the biosynthesis of both compounds, especially the interesting structural features, such as the epoxide or pyrrolidine functionalities in hiroshidine as well as the N−N bond in

the 7-azapteridine scaffold and the oxidation and methylation patterns in taylorflavins.

DISCUSSION

Bioactivity-guided fractionation has long been used to find natural products with the desired properties. Traditional methods, however, have focused on the bioactivity of the "constitutive" metabolome, that is, natural products that are synthesized under standard growth conditions.[35] We now know that constitutively generated natural products are significantly outranked in abundance by the "inducible" metabolome, that is, metabolites induced by generally unknown cues or signals. By combining HiTES with bioactivity assays, our approach allows access to this inducible metabolome resulting from activation of silent BGCs.

We validate Bioactivity-HiTES by reporting cryptic antibiotics from *S. hiroshimensis*. Two of these, taylorflavins A and B, belong to the toxoflavin family of molecules and exhibit the desired bioactivity for which we screened, growth inhibition of *E. coli*. Indeed, taylorflavins were more potent against Gram-negative than Gram-positive bacteria. Because of the selective outer membrane and the hydrolytic enzymes in the periplasmic space, Gram-negative bacteria tend to be less susceptible to antibacterial action by small molecules.[36] Several structural elements of the taylorflavins are likely responsible for their unusual selective phenotype: the taylorflavins are small and are therefore not discriminated against by porins in the outer

membrane of *E. coli*. They do not contain typical structural features that are degraded by well-known hydrolytic enzymes in the periplasm, and the likely target of taylorflavins, the electron transport chain (where toxoflavins act),[37] resides in the inner bacterial membrane, which may be more easily accessed in Gram-negative than in Gram-positive bacteria, due to the extensive peptidoglycan layer in the latter. These features could provide guidelines for designing or finding other potential Gram-negative-selective antibacterial compounds.

Bioactivity-HiTES adds to the available approaches that have similarly leveraged cryptic metabolites in bioactivity assays. Notably, Bachmann and co-workers have used a small number of challenge conditions along with creative eukaryotic reporter assays to identify cryptic metabolites that alter human cell behavior.[23] Co-culture screens have been used by several groups to look for induction of cryptic metabolites with a selected biological activity using agar overlay assays.[38,39] OSMAC-type methods have also been coupled to bioactivity assays to find new, induced metabolites.[40] The differentiating feature of Bioactivity-HiTES is the throughput, as hundreds to thousands of conditions can be examined for induction of cryptic metabolites in a rapid manner. Moreover, the elicitor is linked directly to production of a cryptic, bioactive metabolite, thus enabling downstream mechanistic investigations that can address the basis of the stimulatory activity.

Additional applications of Bioactivity-HiTES are likely to lead to other cryptic metabolites with desired biological properties. The mechanism underlying HiTES is also an emerging area that will gain traction. Our previous applications of HiTES have repeatedly revealed antibiotics as inducers of silent BGCs, highlighting their stimulatory effects at sub-inhibitory concentrations in contrast to inhibitory ones at higher doses.[41] Atenolol, an unsuspected antihypertension medicine, is unlike these previous elicitors in that it does not exhibit growth-inhibitory activity against *S. hiroshimensis*. It not only induced production of the taylorflavins but also generally enhanced the secondary metabolome of *S. hiroshimensis*, which in turn led to the characterization of pyridindolol, two isocoumarins, and hiroshidine. These results indicate that future studies addressing the mode of induction by atenolol will deliver further insights into the regulatory elements that exert cellwide control over secondary metabolism as well as the hormetic functions of antibiotics in *S. hiroshimensis* and beyond.[42]

ASSOCIATED CONTENT

Ⓢ Supporting Information

The Supporting Information is available free of charge on the ACS Publications website at DOI: 10.1021/acschem-bio.9b00049.

Detailed descriptions of materials and methods, including Bioactivity-HiTES, isolation and structural elucidation of cryptic metabolites, bioactivity assays, creation and analysis of gene deletion mutants, Tables S1–S6, and Figures S1–S10 (PDF)

AUTHOR INFORMATION

Corresponding Author
*E-mail: mrseyed@princeton.edu.

ORCID
Mohammad R. Seyedsayamdost: 0000-0003-2707-4854

Notes

ACKNOWLEDGMENTS

REFERENCES

(1) Clardy, J., and Walsh, C. (2004) Lessons from natural molecules. *Nature 432*, 829−837.

(2) Newman, D. J., and Cragg, G. M. (2016) Natural products as sources of new drugs from 1981 to 2014. *J. Nat. Prod. 79*, 629−661.

(3) Cragg, G. M., and Newman, D. J. (2013) Natural products: a continuing source of novel drug leads. *Biochim. Biophys. Acta 1830*, 3670−3695.

(4) Nathan, C. (2004) Antibiotics at the crossroads. *Nature 431*, 899−902.

(5) Bérdy, J. (2005) Bioactive microbial metabolites. *J. Antibiot. 58*, 1−26.

(6) Koehn, F. E., and Carter, G. T. (2005) The evolving role of natural products in drug discovery. *Nat. Rev. Drug Discov. 4*, 206−220.

(7) Projan, S. J. (2003) Why is big Pharma getting out of antibacterial drug discovery? *Curr. Opin. Microbiol. 6*, 427−430.

(8) Bentley, S. D., Chater, K. F., Cerdeño-Tárraga, A. M., Challis, G. L., Thomson, N. R., James, K. D., Harris, D. E., Quail, M. A., Kieser, H., Harper, D., Bateman, A., Brown, S., Chandra, G., Chen, C. W., Collins, M., Cronin, A., Fraser, A., Goble, A., Hidalgo, J., Hornsby, T., Howarth, S., Huang, C. H., Kieser, T., Larke, L., Murphy, L., Oliver, K., O'Neil, S., Rabbinowitsch, E., Rajandream, M. A., Rutherford, K., Rutter, S., Seeger, K., Saunders, D., Sharp, S., Squares, R., Squares, S., Taylor, K., Warren, T., Wietzorrek, A., Woodward, J., Barrell, B. G., Parkhill, J., and Hopwood, D. A. (2002) Complete genome sequence of the model actinomycete *Streptomyces coelicolor* A3(2). *Nature 417*, 141−147.

(9) Ikeda, H., Ishikawa, J., Hanamoto, A., Shinose, M., Kikuchi, H., Shiba, T., Sakaki, Y., Hattori, M., and Omura, S. (2003) Complete genome sequence and comparative analysis of the industrial microorganism *Streptomyces avermitilis*. *Nat. Biotechnol. 21*, 526−531.

(10) Oliynyk, M., Samborskyy, M., Lester, J. B., Mironenko, T., Scott, N., Dickens, S., Haydock, S. F., and Leadlay, P. F. (2007) Complete genome sequence of the erythromycin-producing bacterium *Saccharopolyspora erythraea* NRRL23338. *Nat. Biotechnol. 25*, 447−453.

(11) Nett, M., Ikeda, H., and Moore, B. S. (2009) Genomic basis for natural product biosynthetic diversity in the actinomycetes. *Nat. Prod. Rep. 26*, 1362−1384.

(12) Baltz, R. H. (2017) Gifted microbes for genome mining and natural product discovery. *J. Ind. Microbiol. Biotechnol. 44*, 573−588.

(13) Katz, L., and Baltz, R. H. (2016) Natural product discovery: past, present, and future. *J. Ind. Microbiol. Biotechnol. 43*, 155−176.

(14) Challis, G. L. (2008) Genome mining for novel natural product discovery. *J. Med. Chem. 51*, 2618−2628.

(15) Rutledge, P. J., and Challis, G. L. (2015) Discovery of microbial natural products by activation of silent biosynthetic gene clusters. *Nat. Rev. Microbiol. 13*, 509−523.

(16) Zhu, H., Sandiford, S. K., and van Wezel, G. P. (2014) Triggers and cues that activate antibiotic production by actinomycetes. *J. Ind. Microbiol. Biotechnol. 41*, 371−386.

(17) Ochi, K., and Hosaka, T. (2013) New strategies for drug discovery: activation of silent or weakly expressed microbial gene clusters. *Appl. Microbiol. Biotechnol. 97*, 87−98.

(18) Mao, D., Okada, B. K., Wu, Y., Xu, F., and Seyedsayamdost, M. R. (2018) Recent advances in activating silent biosynthetic gene clusters in bacteria. *Curr. Opin. Microbiol. 45*, 156−163.

(19) Zhang, B., Tian, W., Wang, S., Yan, X., Jia, X., Pierens, G. K., Chen, W., Ma, H., Deng, Z., and Qu, X. (2017) Activation of natural

products biosynthetic pathways *via* a protein modification level regulation. *ACS Chem. Biol. 12*, 1732−1736.

(20) Seyedsayamdost, M. R. (2014) High-throughput platform for the discovery of elicitors of silent bacterial gene clusters. *Proc. Natl. Acad. Sci. U. S. A. 111*, 7266−7271.

(21) Xu, F., Nazari, B., Moon, K., Bushin, L. B., and Seyedsayamdost, M. R. (2017) Discovery of a cryptic antifungal compound from *Streptomyces albus* J1074 using high-throughput elicitor screens. *J. Am. Chem. Soc. 139*, 9203−9212.

(22) Okada, B. K., and Seyedsayamdost, M. R. (2017) Antibiotic dialogues: induction of silent biosynthetic gene clusters by exogenous small molecules. *FEMS Microbiol. Rev. 41*, 19−33.

(23) Earl, D. C., Ferrell, P. B., Jr., Leelatian, N., Froese, J. T., Reisman, B. J., Irish, J. M., and Bachmann, B. O. (2018) Discovery of human cell selective effector molecules using single cell multiplexed activity metabolomics. *Nat. Commun. 9*, 39.

(24) Xu, F., Wu, Y., Zhang, C., Davis, K. M., Moon, K., Bushin, L. B., and Seyedsayamdost, M. R. (2019) A genetics-free method for high-throughput discovery of cryptic microbial metabolites. *Nat. Chem. Biol. 15*, 161−168.

(25) van Damme, P. A., Johannes, A. G., Cox, H. C., and Berends, W. (1960) On toxoflavin, the yellow poison of *Pseudomonas cocovenenans. Recl. Trav. Chim. Pays-Bas 79*, 255−267.

(26) Miller, T. W., Chaiet, L., Arison, B., Walker, R. W., Trenner, N. R., and Wolf, F. J. (1963) Isolation and characterization of antibiotic MSD-92, a pyrimidotriazine antibiotic. *Antimicrob. Agents Chemother. 161*, 58−62.

(27) Taylor, E. C., and Sowinski, F. (1969) Structure and total synthesis of the pyrimido(5,4-e)-as-tri-azine antibiotic, 2-methylfervenulone. *J. Am. Chem. Soc. 91*, 2143−2144.

(28) Taylor, E. C. (1993) Design and synthesis of inhibitors of folate-dependent enzymes as antitumor agents. *Adv. Exp. Med. Biol. 338*, 387−408.

(29) Aoyagi, T., Kumagai, M., Hazato, T., Hamada, M., Takeuchi, T., and Umezawa, H. (1975) Pyridindolol, a new beta-galactosidase inhibitor produced by actinomycetes. *J. Antibiot. 28*, 555−557.

(30) Zinad, D. S., Shaaban, K. A., Abdalla, M. A., Islam, M. T., Schüffler, A., and Laatsch, H. (2011) Bioactive isocoumarins from a terrestrial *Streptomyces* sp. ANK302. *Nat. Prod. Commun. 6*, 45−48.

(31) Wu, C., Du, C., Ichinose, K., Choi, Y. H., and van Wezel, G. P. (2017) Discovery of C-glycosylpyranonaphthoquinones in *Streptomyces* sp. MBT76 by a combined NMR-based metabolomics and bioinformatics workflow. *J. Nat. Prod. 80*, 269−277.

(32) Fenwick, M. K., Philmus, B., Begley, T. P., and Ealick, S. E. (2011) Toxoflavin lyase requires a novel 1-His-2-carboxylate facial triad. *Biochemistry 50*, 1091−1100.

(33) Philmus, B., Shaffer, B. T., Kidarsa, T. A., Yan, Q., Raaijmakers, J. M., Begley, T. P., and Loper, J. E. (2015) Investigations into the biosynthesis, regulation, and self-resistance of toxoflavin in *Pseudomonas protegens* Pf-5. *ChemBioChem 16*, 1782−1790.

(34) Fenwick, M. K., Philmus, B., Begley, T. P., and Ealick, S. E. (2016) *Burkholderia glumae* toxA is a dual-specificity methyltransferase that catalyzes the last two steps of toxoflavin biosynthesis. *Biochemistry 55*, 2748−2759.

(35) Bachmann, B. O., Van Lanen, S. G., and Baltz, R. H. (2014) Microbial genome mining for accelerated natural products discovery: is a renaissance in the making? *J. Ind. Microbiol. Biotechnol. 41*, 175−184.

(36) Silhavy, T. J., Kahne, D., and Walker, S. (2010) The bacterial cell envelope. *Cold Spring Harb. Perspect. Biol. 2*, a000414.

(37) Latuasan, H. E., and Berends, W. (1961) On the origin of the toxicity of toxoflavin. *Biochim. Biophys. Acta 52*, 502−508.

(38) Pettit, R. K. (2009) Mixed fermentation for natural product drug discovery. *Appl. Microbiol. Biotechnol. 83*, 19−25.

(39) Seyedsayamdost, M. R., Traxler, M. F., Clardy, J., and Kolter, R. (2012) Old meets new: using interspecies interactions to detect secondary metabolite production in actinomycetes. *Methods Enzymol. 517*, 89−109.

(40) Bode, H. B., Bethe, B., Höfs, R., and Zeeck, A. (2002) Big effects from small changes: possible ways to explore nature's chemical diversity. *ChemBioChem 3*, 619−627.

(41) Rosen, P. C., and Seyedsayamdost, M. R. (2017) Though much is taken, much abides: finding new antibiotics using old ones. *Biochemistry 56*, 4925−4926.

(42) Davies, J., Spiegelman, G. B., and Yim, G. (2006) The world of subinhibitory antibiotic concentrations. *Curr. Opin. Microbiol. 9*, 445−453.